Direct Contact-Area Computation for MEMS Using Real Topographic Surface Data

Daniel J. Dickrell, III, *Member, ASME*, Michael T. Dugger, *Member, ASME*, Matthew A. Hamilton, and W. Gregory Sawyer, *Member, ASME*

***Abstract*—Direct computation of interfacial contact area for microelectromechanical-system applications was performed numerically using the measured device surface topography and the material hardness to define the flow stress of an individual element. The simulation results compared well with the established contact-area determination methods and also introduced new capabilities that enabled the visualization of the spatial distribution of contact spots to be computationally mapped and rendered directly onto device surfaces. [2006-0276]**

***Index Terms*—Contact mechanical factors, contacts, friction.**

I. Introduction

INTERFACIAL contact-area determination is very important for microelectromechanical-system (MEMS) device design. The phenomena that affect the MEMS device performance and lifetime are primarily dependent on the interaction area between device surfaces (examples include surface adhesion, friction, wear, and electrical contact resistance). The gross contact geometry of most MEMS electrical switches is planar, which stems from the layered fabrication processes that are used to create the device. The actuation forces in the operation of MEMS contacts are typically on the order of 10–100 μN. The local surface roughness mainly determines the real area of contact as very few asperity contacts are required to support these loads [1], [2]; the real area of contact is likely orders-of-magnitude smaller than the apparent area of contact, as defined by the device design. The combination of low contact forces and nominally flat contact geometry accentuates this subtle influence of the surface-roughness variation on device contact-area spot size and distribution. An accurate determination of interfacial contact area in MEMS requires proper surface-roughness characterization and appropriate uses of these measurements to predict contact-area size and distribution under these extremely low force operating conditions.

Fig. 1(a) and (b) shows the characteristic roughness exhibited by a MEMS device contact surface. Fig. 1(a), which is obtained by scanning electron microscopy, shows the overall planar geometry of a contact dimple that is patterned on the tip of a gold-coated cantilever structure. The locations somewhere within the area, shown in Fig. 1(a), will carry the mechanical load caused by device operation. The rough surface topography shown in Fig. 1(b), which is obtained by atomic force microscopy (AFM), represents the potential locations of individual contact islands that make up the interfacial contact area formed in response to an applied operation force. Modern surface imaging capabilities such as AFM enable a detailed reckoning of the MEMS device topography that can be used to calculate the interfacial contact area.

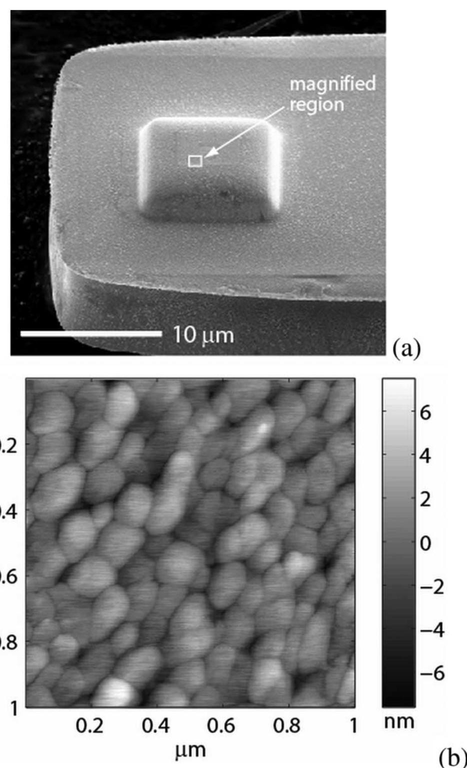

Fig. 1. (a) and (b) Example of a rough surface in a MEMS device, which is, in this case, a contact dimple on the bottom of a cantilever switch. (b) Surface shown in the magnified view is an evaporatively deposited gold having a measured average and root-mean-squared roughness of 1.37 and 1.71 nm, respectively.

One of the earliest calculation methods of the interfacial contact area formed by two interacting bodies was developed by Hertz [3]. This approach assumed a completely elastic contact and neglected any effect of surface roughness on the interfacial contact area. Even though the Hertzian approach neglects the surface-roughness effects completely, it is still currently used

Manuscript received December 13, 2006; revised April 9, 2007. Sandia is a multiprogram laboratory operated by Sandia Corporation, a Lockheed Martin Company, for the United States Department of Energy's National Nuclear Security Administration under Contract DE-AC04-94AL85000. Subject Editor L. Lin.

D. J. Dickrell, III, M. A. Hamilton, and W. G. Sawyer are with the Department of Mechanical and Aerospace Engineering, University of Florida, Gainesville, FL 32611 USA (e-mail: djd3@ufl.edu).

M. T. Dugger is with the Microsystem Materials Department, Sandia National Laboratories, Albuquerque, NM 87185 USA.

Digital Object Identifier 10.1109/JMEMS.2007.901120

1057-7157/$25.00 © 2007 IEEE

to explain the device behavior of both silicon and metal-coated surfaces due to its simplicity and popularity [4].

Full plasticity approaches to treat the contacting surfaces attempt to resolve the mechanical contact area of the interacting surfaces using only material hardness and normal load. This assumption implies that real contact area is only related to the applied load F_{n} and the material indentation hardness H and is completely independent of contact geometry [5]. This approach ignores any effect surface-roughness contributions to the contact-area calculation. Equation (1) shows this simple expression for contact area A_{c}, assuming only plastic deformation of the surfaces. Both the Hertzian and the plastic contact material models neglect any effect of surface roughness on the contact area

$$A_{\mathrm{c}} = \frac{F_{\mathrm{n}}}{H}. \quad (1)$$

Due to the rough nature of surfaces, it is widely recognized that the real area of contact is a collection of discrete contact events that are distributed across a surface. One of the more widely cited approaches that captured this effect was developed by Greenwood and Williamson (G–W). The G–W model proposed a statistically based asperity contact model based on the separation of a deformable rough surface that is composed of perfectly spherical asperities and an ideally smooth rigid plane [6]. From the relative interference between the rigid plane and the rough surface, it was possible to compute the resultant contact area and load supported by knowing the height distribution of surface asperities, their size, and their material composition. The key assumptions of this model were that all asperities in contact were spherical and had the same radius of curvature, that there was no interaction between neighboring asperities, and that the asperity heights followed a continuous statistical distribution (assumed to be normally distributed).

Succeeding refinements to the G–W model relaxed some of the key assumptions used in its formulation. The numerically simulated surface contacts incorporated the anisotropically distributed elliptically paraboloidal asperities. These simulation results differed only slightly from that produced by the G–W model and that the elastic contact of rough bodies could be used to bound the contact-area-dependent properties such as electrical contact resistance [7]–[9]. Thus, these subsequent studies demonstrated that the G–W model was a good approximation for the two contacting rough surfaces even though its assumptions are not overly complex, as long as the asperity-height distribution is statistically valid for the surfaces under consideration.

For the MEMS applications, the reliance of statistically based contact models on good correlation between a mathematical function and the contact surface topography becomes tenuous. As long as the assumed analytical fitting function adequately approximates the asperity-height histogram, for example at sufficiently high normal loads that involve a significant fraction of asperities, the statistically based contact models like G–W are suited for the contact-area prediction. When the contact load is reduced so that the penetration distance is small with respect to the surface roughness, and therefore a small fraction of surface points are sufficient to support the normal load, then the correspondence between the fitted height distribution and the real contact surface diverges. For instances of low force rough surface contact, an alternative to statistical arguments of surface roughness in interfacial area calculation is desirable.

The most direct approach to calculate the rough surface contact area is to use the 3-D discretized surface data obtained from surface microscopy, without assumptions of modifications regarding the surface topography, to obtain contact area for a given force. Quantitative discretized surface data are most often obtained from stylus profilometry, optical profilometry, or AFM, depending on the scan area size and range of surface heights to be measured. Such devices are capable of accurately measuring the surface height data quickly and without an extensive sample preparation and experimental setup time. The utility and accuracy of such surface topography tools offer a comprehensive topographical rendering of a functional contact surface, negating the necessity for simplifying the statistical assumptions regarding surface data. This is in contrast to treatments that input the topographic measurements to construct model surfaces that are used in the contact-area calculation. For example, finely meshed finite-element simulations of contacting rough surfaces are capable of evaluating the contact area of arbitrary surfaces [10]. Unfortunately, finite-element approaches often require hours of computational time to obtain a result and are sensitive to ill-conditioned surface profiles. The utility of computationally intensive contact-area calculation methods in an industrial engineering setting is therefore limited.

This paper proposes a method to use the real surface topography to directly compute the interfacial contact area for engineering surfaces of interest, and MEMS contacts particularly, in a rapid and reasonably accurate fashion that is specifically useful to engineering interests.

II. Contact Modeling

Engineering surfaces of interest are discretized into a collection of voxels, or volume pixels, shown in Fig. 2(a) and (b), and are frequently rendered as pixels in 2-D height maps [Fig. 1(b)]. The voxel rough surface model is composed of a collection of individual of voxels, with each voxel representing a Z-value at a single surface location in a numerical array that encompasses the surface topography relative to all points measured by the method. The Z-height is computed from a reference datum plane, which is usually taken as the arithmetic mean of all of the surface heights. All of the voxels have the same cross-sectional area, which may or may not be square and is determined by the spatial resolution of the measuring device that is used to obtain the topographic data. Each voxel in the array is independent of its neighbor voxels, and the material response of each voxel to mechanical load does not communicate to the neighboring voxels.

To calculate the interfacial contact area, two voxel surfaces are placed in a distance that is far away from each other. The surfaces are then advanced toward one another until, at some surface separation, the voxel elements begin to interfere. Fig. 2(a) shows two voxelized surfaces that are about to be brought into contact. As the surface separation decreases, the number of voxels intersecting (contact) increases. If the voxels

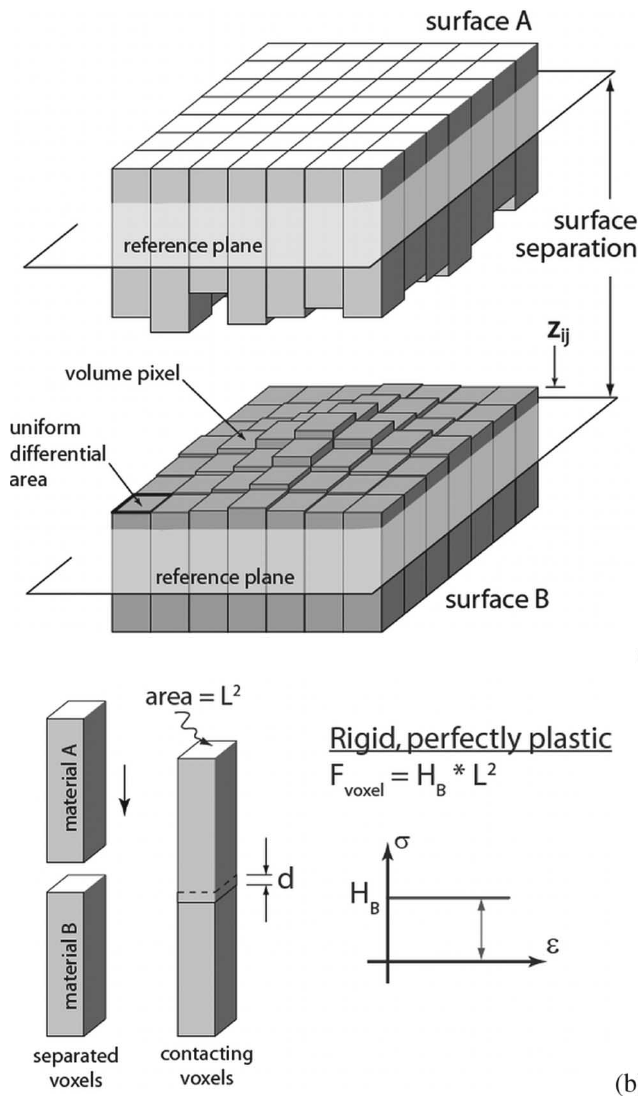

Fig. 2. (a) and (b) Voxel surface contact between the two surfaces and the constituative material model used to calculate the load-carrying capacity of an individual voxel contact.

have a uniform differential area of L^2, where L represents the linear dimension of one square pixel in the surface scan, then the surface contact area is composed of the summation of all of the individual voxel encounters occurring at a given surface separation multiplied by L^2.

The calculation of the load-carrying capacity of an individual voxel is performed by using a rigid perfectly plastic material model to govern the relation of voxel interference (strain) to pressure (stress). This assumption states that no elastic strain is built up as the voxels are pressed together and the contact pressure is always equal to the material indentation hardness. Fig. 2(b) shows the stress–strain relation for the rigid perfectly plastic material assumption.

The contact force generated from a single voxel interaction is calculated from the material indentation hardness of the softer material in contact and the area of the voxel. By rearranging the expression shown in (1) to express force in terms of indentation hardness and contact area, each voxel in contact contributes the same increment of load support, shown in (2), regardless of the degree of deformation of the voxel. The force for the entire contact is calculated by summing the force contributions from the N interacting voxel pairs, which is shown in (3)

$$F_{\rm voxel} = H * L^2 \tag{2}$$

$$F_{\rm n} = \sum_{i=1}^{N} F_{{\rm voxel}_i}. \tag{3}$$

The rigid perfectly plastic assumption circumvents the need to define the elastic strain for each individual element with respect to an arbitrary gage length. A more rigorous voxel contact modeling approach would incorporate an elastoplastic material behavior as well as the volumetric redistribution of the material displaced inside the contact as the material plastically flows outward to nonstressed areas. Numerical simulation of a perfect sphere-on-flat contact with this refinement showed that the force–displacement response of the refined voxel contact model was compressed by almost 50%. This occurred due to the smaller displacement required to reach the target load that is caused by the migration of plastically deformed volume to neighboring voxels and contribution to the load support. However, only the surface-separation distance required to reach the target load was affected, and the overall contact area did not change substantially. The number of voxels required to support the load remained the same. The inclusion of intervoxel communication via mass redistribution was therefore neglected in the voxel contact model since the calculation of contact-area size was of primary concern. The drawback to mass-redistribution inclusion was the increased computational time required to locate the neighbor voxel elements. The increase in time directly negated the computational advantage of the noninteracting voxel contact method: The voxels of one surface are directly registered to the voxels in the opposing surface, and no computationally expensive neighbor searching was required to locate the contacting voxel elements. This computational economy allowed for almost real-time calculations of contact areas for relevant engineering surfaces at the expense of force–displacement relationship accuracy.

To compare the voxel contact-area calculation method with more traditional approaches, an initial test was performed by applying the aforementioned method on two rough surfaces, a 0.79-mm radius gold-coated Si_3N_4 sphere and a gold-coated silicon wafer, at an applied load where a statistical treatment of surface roughness would be appropriate. Scanning-white-light interferometric topography scans of the surfaces are shown in Fig. 3(a)–(c). The indentation hardness used for the contact force calculation was 1.9 $\pm$ 0.3 GPa, which was determined from the nanoindentation hardness testing of the same deposited material. The measured elastic modulus used for elastic model comparison was 78 $\pm$ 3 GPa.

Contact simulation was performed by decrementing the distance between the surfaces until the calculated contact force became nonzero. The surface separation was then reduced in increments of 0.2 nm until the calculated contact force became equal to the target contact force. When the target contact force was reached, the contact area was determined from the sum of interacting voxels which supported the target force.

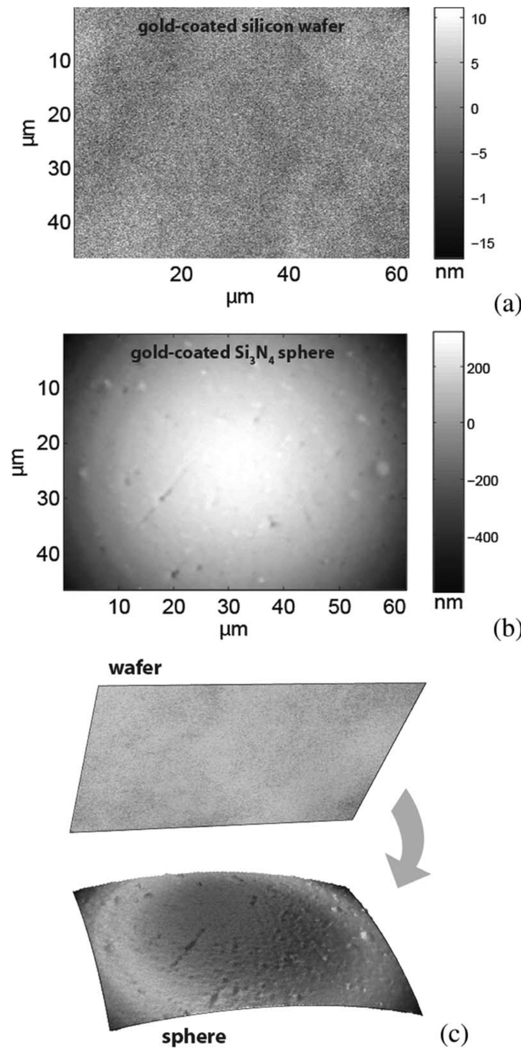

Fig. 3. (a)–(c) Voxel surfaces obtained from the scanning-white-light interferometry. (a) Flat and (b) ball surfaces are voxel arrays of 640 × 480 pixels with corresponding Z-heights about their surface mean. Each square pixel had a side length of 97 nm. The two surfaces were numerically brought into contact to calculate the interfacial contact area.

The contact-area results for a 60-mN target normal load using the voxel calculation method are shown in Fig. 4. The total area determined by the voxel method was 30.7 μm^2, having an equivalent circular contact-spot radius of 3.13 μm. Also shown in Fig. 4 are the contact-area results obtained using the "gold-standard" Hertzian and G–W methods for the same target load of 60 mN [3], [11]. The gray area shown in Fig. 4 spans the range of areas obtainable by altering one of the statistical input parameters in the G–W model, which is the average asperity radius of curvature β, from 100 nm for the smaller area to 1 μm for the larger. The effective contact areas were 18.3 and 57.9 μm^2 for the 100 nm and 1 μm radius of curvatures, respectively. The standard deviation of the asperity-height distribution was chosen to be 5 nm, although significant freedom exists also in the determination of what consists of an "asperity" and distribution about the height mean [12].

While the Hertzian and the G–W calculation methods are both capable of predicting the contact size, neither the Hertzian or the G–W method is capable of predicting the spatial distribution of lesser contact spots within the greater contact area itself. The capability of the voxel method to compute both contact-area magnitude and local spatial distribution is useful when the spatially distribution dependent properties, such as electrical contact resistance and thermal conduction, are to be considered.

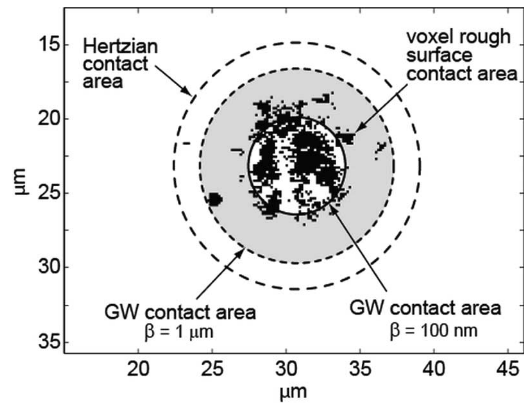

Fig. 4. Contact areas calculated using the voxel, Hertzian, and G–W methods. One notable aspect of the voxel method is the visualization of minor contact spots within the larger contact area. This information is not obtainable with the Hertzian and G–W methods which only compute the effective circular spot area.

III. Discussion

The previous section demonstrated that the voxel contact method, although based on very simple material arguments, yielded a contact-area result that is comparable to what was obtained with some of the most widely utilized methods, which are the Hertzian contact and the G–W model size for a macroscale contact. However, the unique nature of MEMS contacts, with very lightly loaded surface interactions, does not readily lend themselves to the use of traditional contact-area calculation methods where surface roughness is less influential. An example of the utility of the voxel-based approach in the MEMS contact-area calculation is shown in Fig. 5(a)–(c). The same numerical procedure used to generate the contact area in Fig. 4 was used to find the contact area, shown in Fig. 5(c), which is produced by two gold MEMS device surfaces subjected to a load of 1.5 μN.

The irregular surface topography obtained by AFM scanning represents the characteristic length scale which determines how the MEMS device surface interactions perform. Operational friction, wear, and adhesion behaviors stem from the details of how such rough surfaces interact. Using the measured surface topography directly to calculate the interfacial contact, instead of idealized models, seems logical as the ability to obtain high-resolution surface topographical data from the areas of interest advances.

The use of this approach in a real MEMS design setting must be modified to account for the lack of specific knowledge of registration between the device surfaces. For example, sequential application of the voxel contact method using first the total area of potential contact shown in Fig. 1(a) would identify the potential areas of contact with limited spatial resolution. A second topographic scan that is taken at higher resolution

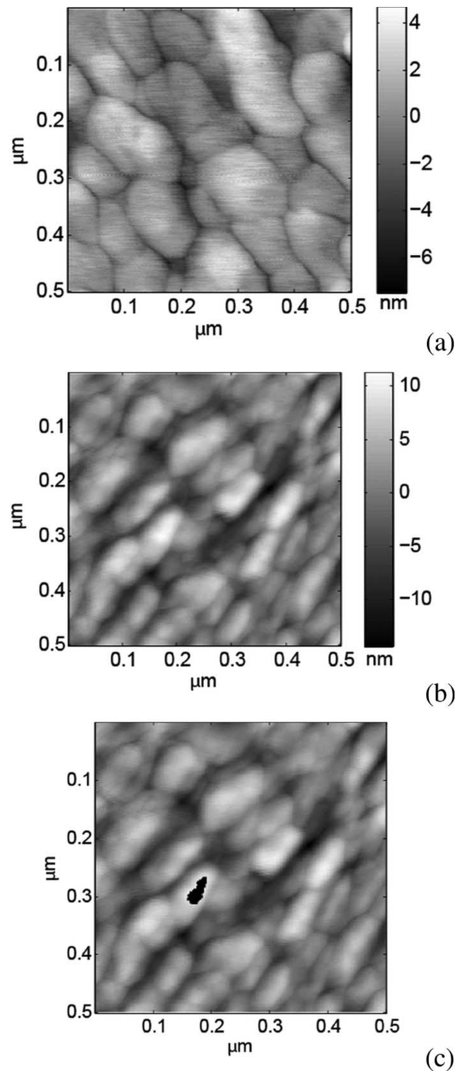

Fig. 5. (a)–(c) Voxel surface contact for the MEMS electrical contact surfaces subjected to a 1.5-μN load. The contact area was generated by the interaction of the surfaces shown in (a) and (b), and it is shown in (c) as a single black island which measures approximately 30 × 50 nm. The material hardness used for the voxel simulation was 2 GPa.

centered about the region identified in the coarser topographic scan, shown in Fig. 1(b), would be used to calculate a spatially refined contact-area result. Alternatively, the entire contact surface could be imaged and numerically stitched together to form a high-resolution voxel surface model that is used to calculate the contact area in a single computational step. Either approach refinement is achievable with available surface imaging tools such as AFM that is capable of bridging the length scales required.

A number of major limitations remain in such direct treatments of surface contact. One limitation is that the far-field elastic deformations and flexibilities are not modeled, and thus, the contact patches do not necessarily provide static equilibrium. Another limitation is that the surface scans must be fine enough to capture a finite number of contact events; the minimum contact area of this model is L^2. The redistribution of the displaced material is expected to result in a real contact area that increases more rapidly with an applied load than in the present case. This method strikes a balance between the rigor of using the actual surface topographic measurements and the mathematical simplicity of directly intersecting the discretized surfaces. Finally, this method is not meant to "reinvent the wheel" with respect to the underlying foundation of contact mechanics but to show how the combination of surface analytical tools and numerical computation was not available to earlier investigators can quickly and accurately estimate the interfacial contact area of real engineering surfaces.

IV. Conclusion

The voxel contact area calculation method outlined previously is preferable to the statistical contact area methods such as G–W for lightly loaded contact between rough surfaces, which is due to the absence of assumptions about asperity shape and distribution. The quantitative topographic data taken from two surfaces of interest can be used to directly compute the predicted contact area using the straightforwardly obtained material constants and simple constituative models. The voxel rough surface contact model also allows for predictions in contact-area shape, which is an ability that is completely lacking in the statistically based models. The resulting prediction of contact-area size and spatial distribution can be used to help explain the low-force electrical contact and thermal phenomena for the MEMS applications.

Acknowledgment

D. J. Dickrell and M. T. Dugger would like to thank T. Buchheit of Sandia National Laboratory for the experimental nanoindentation support.

References

[1] S. Majumder, N. E. McGruer, G. G. Adams, P. M. Zavracky, R. H. Morrison, and J. Krim, "Study of contacts in an electrostatically actuated microswitch," *Sens. Actuators A, Phys.*, vol. 93, no. 1, pp. 19–26, Aug. 2001.

[2] J. Schimkat, "Contact measurements providing basic design data for microrelay actuators," *Sens. Actuators A, Phys.*, vol. 73, no. 1, pp. 138–143, Mar. 1999.

[3] K. L. Johnson, *Contact Mechanics*. London, U.K.: Cambridge Univ. Press, 1998.

[4] Y. Shi and S. G. Kim, "A lateral, self-cleaning, direct-contact MEMS switch," in *Proc. 18th IEEE Int. Conf. MEMS*, 2005, pp. 195–198.

[5] R. Holm, *Electric Contacts: Theory and Application*. New York: Springer-Verlag, 1967.

[6] J. A. Greenwood and J. P. B. Williamson, "Contact of nominally flat surfaces," *Proc. R. Soc. Lond. A, Math. Phys. Sci.*, vol. 295, no. 1442, pp. 300–319, 1966.

[7] J. I. McCool, "Comparison of models for the contact of rough surfaces," *Wear*, vol. 107, no. 1, pp. 37–60, 1986.

[8] A. W. Bush, R. D. Gibson, and T. R. Thomas, "The elastic contact of a rough surface," *Wear*, vol. 35, no. 1, pp. 87–111, 1975.

[9] J. R. Barber, "Bounds on the electrical contact resistance between contacting elastic rough bodies," *Proc. R. Soc. Lond. A, Math. Phys. Sci.*, vol. 459, no. 2029, pp. 53–66, 2003.

[10] S. Hyun, L. Pei, J.-F. Molinari, and M. O. Robbins, "Finite-element analysis of contact between elastic self-affine surfaces," *Phys. Rev. E, Stat. Phys. Plasmas Fluids Relat. Interdiscip. Top.*, vol. 70, no. 2, p. 026 117, Aug. 2004.

[11] B. Bhushan and M. T. Dugger, "Real contact area measurements on magnetic rigid disks," *Wear*, vol. 137, no. 1, pp. 41–50, 1990.

[12] J. A. Greenwood and J. J. Wu, "Surface roughness and contact: An apology," *Meccanica*, vol. 36, no. 6, pp. 617–630, 2001.